Bao-kai WANG, Martina BARBIERO, Qi-ming ZHANG, Min GU, 2019. Super-resolution optical microscope: principle, instrumentation, and application. *Frontiers of Information Technology & Electronic Engineering,* 20(5):608-630. https://doi.org/10.1631/FITEE.1800449

Super-resolution optical microscope: principle, instrumentation, and application

Key words: Super-resolution; Imaging; Optical microscope

Corresponding author: Min GU
E-mail: gumin@usst.edu.cn
ORCID: http://orcid.org/0000-0003-4078-253X

Introduction

1. Over the past two decades, several fluorescence- and non-fluorescence-based optical microscopes have been developed to break the diffraction limited barrier.

2. In this review, the basic principles implemented in microscopy for super-resolution are described.

3. Furthermore, achievements and instrumentation for super-resolution are presented.

4. In addition to imaging, other applications that use super-resolution optical microscopes are discussed.

Principle: fluorescence-based super-resolution

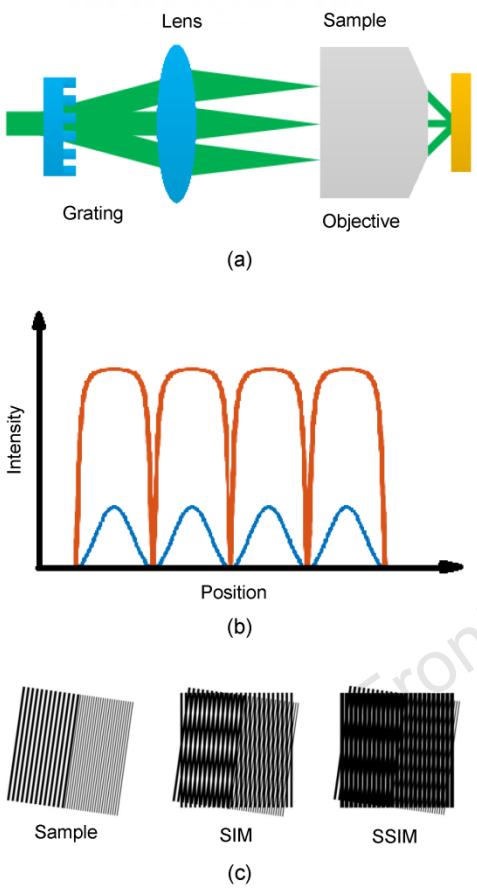

Fig. 1 Principles of structured-illumination microscopy (SIM) and saturated structured-illumination microscopy (SSIM): (a) structured illumination generated by a grating; (b) SIM excitation pattern (blue line) and SSIM excitation pattern (red line); (c) imaging the sample with SIM and SSIM

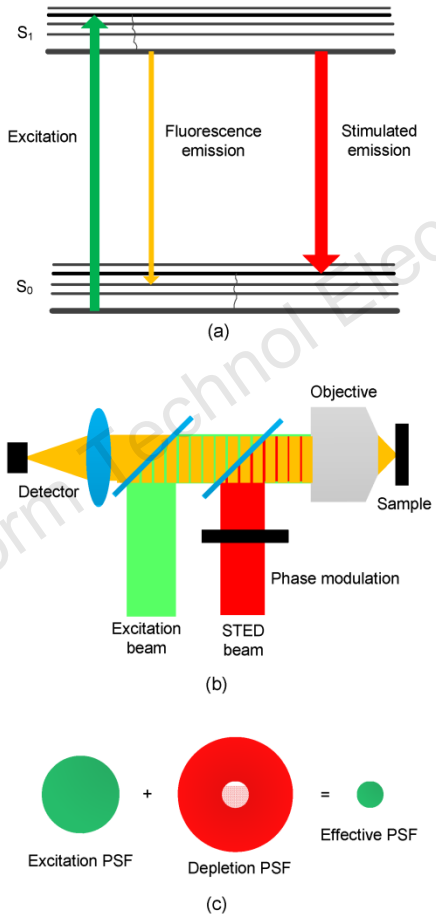

Fig. 2 Principle of the stimulated emission depletion (STED) microscope: (a) Jablonski diagram of the process of fluorescence emission and stimulated emission; (b) schematic of an STED microscope; (c) effective point spread function (PSF) generated

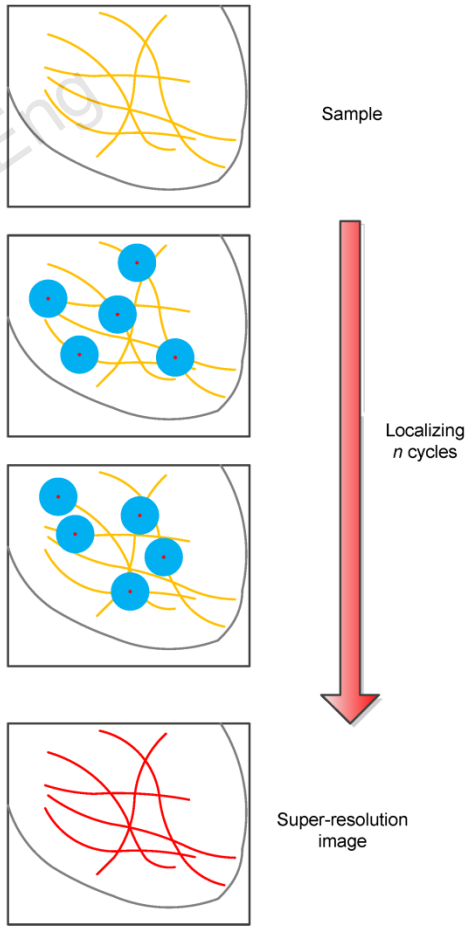

Fig. 6 Principles of photoactivated localization microscopy (PALM), stochastic optical reconstruction microscopy (STORM), blinking localization, 3B analysis, and ground state depletion microscopy followed by individual molecule return (GSDIM)

Principle: fluorescence-based super-resolution (Cont'd)

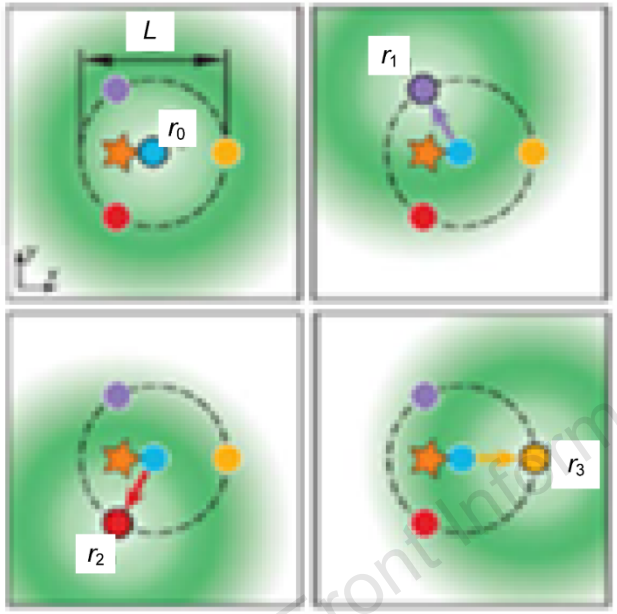

Fig. 7 Localization of one molecule with four positions
The star represents the target emitter. The four points are the central positions of the doughnuts. The fluorescent signals from these four positions are used to localize the target emitter. Reprinted from Balzarotti et al. (2017), Copyright 2017, with permission from the American Association for the Advancement of Science

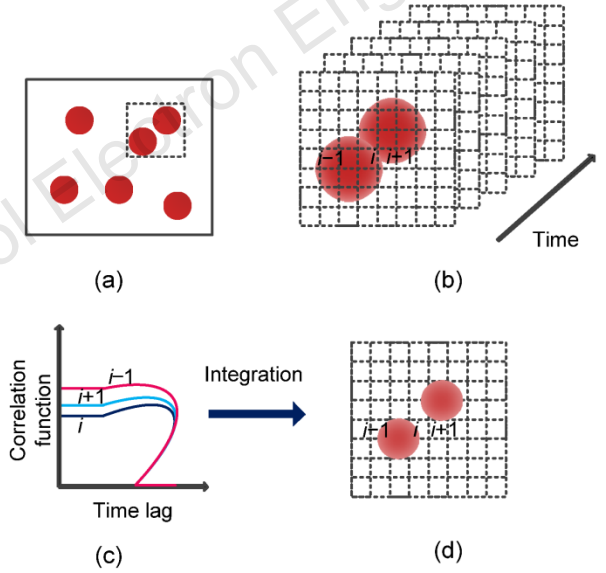

Fig. 8 Principle of super-resolution optical fluctuation imaging (SOFI): (a) wide-field imaging; (b) a movie recoding two fluorescent probes in three neighboring pixels; (c) second-order correlation function calculated for each pixel; (d) SOFI intensity value for each pixel

Principle: non-fluorescence-based super-resolution

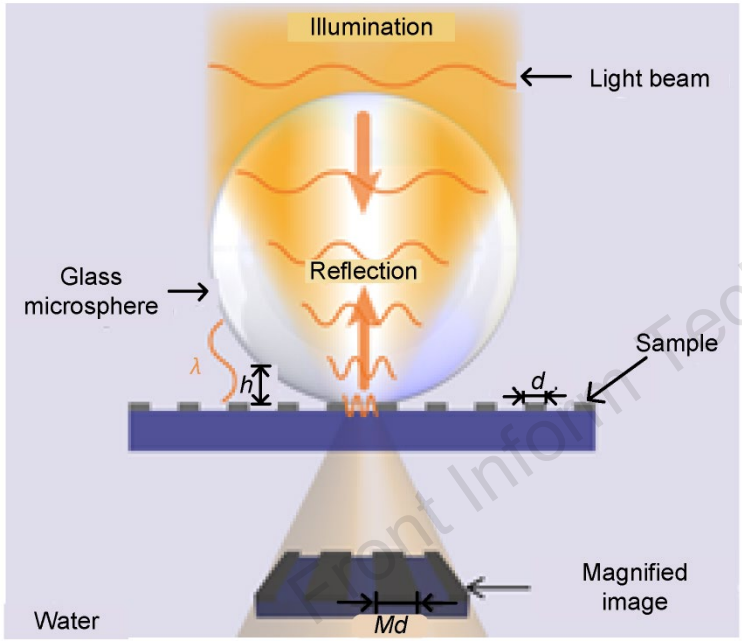

Fig. 9 Super-resolution imaging with a dielectric microsphere
One dielectric microsphere is placed on a grating (line width is *d*) and illuminated from the front. The reflected light from the grating allows detection of a magnified virtual image (magnification factor is *M*). When the distance *h* between the microsphere and the grating is small enough (of order of the illumination wavelength λ), the near-field evanescent wave carrying the high-frequency information begins propagating in the high refractive-index sphere, and is then collected by the microscope objective. Reprinted from Yang et al. (2016), Copyright 2016, with permission from American Chemical Society

Highlighted achievement: multicolor imaging and live-cell imaging

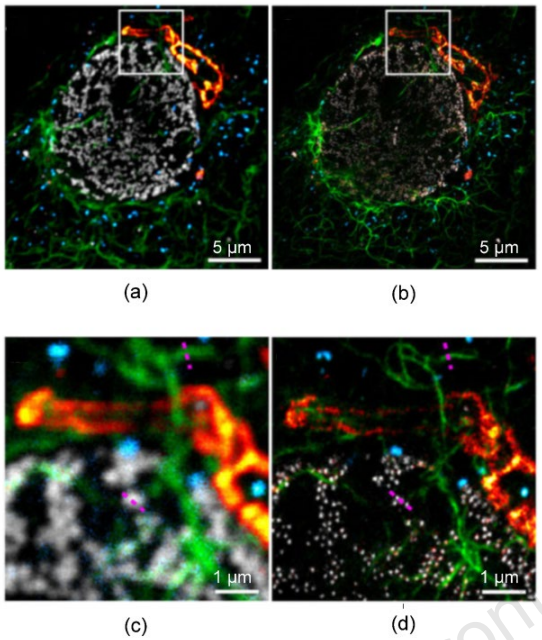

Fig. 10 Four-color stimulated emission depletion (STED) imaging of a fixed cell: (a) confocal overlay; (b) STED overlay; (c) enlarged view of the region in the white square in (a); (d) enlarged view of the region in the white square in (b)

Excitation wavelength is 612 nm; STED wavelength is 775 nm. The fluorescence is detected by a hyperspectral detection design spanning a total range of 620–750 nm in four channels (blue: peroxisomes–Atto594; green: vimentin–Abberior Star635P; red hot: giantin–KK1441; grey: nuclear pores–CF680R) (Winter et al. (2017), licensed under CC BY 4.0). References to color refer to the online version of this figure

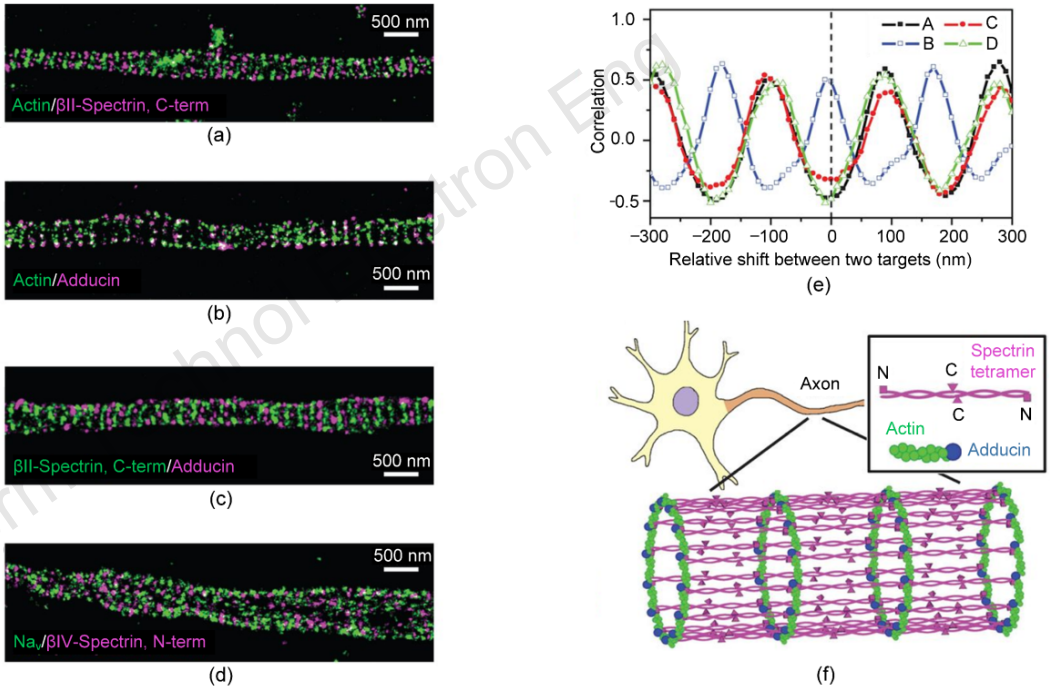

Fig. 11 Two-color STORM imaging of actin, spectrin, adducin, and sodium channels: (a) two-color STORM image of actin (green) and βII-spectrin (magenta); (b) two-color STORM image of actin (green) and adducin (magenta); (c) two-color STORM image of βII-spectrin (green) and adducin (magenta); (d) two-color STORM image of sodium channels (Na$_v$, green) and βIV-spectrin (magenta); (e) spatial correlations between actin and the βII-spectrin C terminus [(A), black], between actin and adducin [(B), blue], between adducin and the βII-spectrin C terminus [(C), red], and between sodium channels and the βIV-spectrin N terminus [(D), green]; (f) a model for the cortical cytoskeleton in axons

βII-spectrin is immunostained against its C-terminal region, which is situated at the center of the spectrin tetramer. βIV-spectrin is immunostained against its N-terminal region, which is situated at the two ends of the spectrin tetramer. Short actin filaments (green), capped by adducin (blue) at one end, form ringlike structures wrapping around the circumference of the axon. Spectrin tetramers (magenta) connect the adjacent actin/adducin rings along the axon, creating a quasi-1D lattice structure with a periodicity of about 180 to 190 nm. Reprinted from Xu et al. (2013), Copyright 2013, with permission from the American Association for the Advancement of Science. References to color refer to the online version of this figure

Instrumentation

Table 1 Specifications of microscopes based on structured-illumination microscopy (SIM)

Company	Product	Lateral resolution (nm)	Axial resolution (nm)	Acquisition speed	Camera	Number of colors
Nikon	N-SIM	85–115	300	0.6–1.0 s/frame (1–2 s for calculation)	EMCCD	5
Zeiss	ELYRA S.1	120	300	1.5–1.6 s/frame	EMCCD	2
Olympus	SpinSR10	120	X	5 ms/frame	CMOS	2

Table 2 Specifications of microscopes based on stimulated emission depletion (STED)

Company	Product	Lateral resolution (nm)	Axial resolution (nm)	STED wavelength (nm)	Excitation wavelength (nm)	Number of colors
Leica	Leica TCS SP8	30–80	130	592, 660, 775	Up to 8 wavelengths	5
Abberior	775 STED	20–30	Confocal	775	594, 640	2
Abberior	595 STED	25–40	Confocal	595	488, 518	2
Abberior	Easy3D STED	75–100	75–100	775	594, 640	3

Instrumentation

Table 3 Specifications of microscopes based on stochastic optical reconstruction microscopy (STORM), photoactivated localization microscopy (PALM), and ground state depletion microscopy followed by individual molecule return (GSDIM)

Company	Product	Lateral resolution (nm)	Axial resolution (nm)	Maximum field of view (μm)	Acquisition speed	Camera	Number of colors
Bruker	Vutara 352	20	50	40×40	Up to 3000 frames/s	sCMOS	2
ONI	Nanoimager	20	50	50×80	100 frames/s for full frame and 5 kHz with frame height cropped to 2%	sCMOS	2
Nikon	N-STORM 5.0	20	50	80×80	Up to 500 Hz	sCMOS	3
Zeiss	ELYRA P.1	20	50–80	81.1×81.1	30 frames/s for full frame and >100 frames/s in sub-array mode	EMCCD	3
Leica	Leica SR GSD 3D	20	50	40×40	Over 1000 frames/s	sCMOS	3

Table 4 Specifications of microscopes based on reversible saturable optically linear fluorescence transitions (RESOLFT)

Company	Product	Lateral resolution (nm)	Optical system	Doughnut number	Number of colors
Abberior	RESOLFT	<70	Point scanning	1	2
Abberior	2-color RESOLFT parallel	<80	Wide-field	>100 000	2

Other applications

1. Three-dimensional sub-diffraction optical laser lithography
2. Magnetic imaging

Summary

1. We reviewed the principles of various super-resolution microscopes, including fluorescence- and non-fluorescence-based methods.

2. We also present the status of instrumentation of super-resolution microscopes and compare the specifications of commercial products.

3. Inspired by super-resolution methods in STED microscopy, three SPIN methods were developed and enabled 3D nanofabrication with application in optical data storage. Super-resolution optical magnetic imaging is also very promising as a new tool to understand biological processes.